Full Paper

A New Electrochemical Sensor for the Simultaneous Detection of Morphine and Methadone based on Thioglycolic Acid Decorated CdSe Doped Graphene Oxide Multilayers

Zahra Nazari, and Zarrin Es'haghi*

Department of Chemistry, Payame Noor University, 19395-4697, Tehran, Iran

*Corresponding Author, Tel.: +9838683004

E-Mail: eshaghi@pnu.ac.ir

Abstract- In this study, an electrochemical sensitive sensor based on thioglycolic acid decorated cadmium selenide (CdSe) doped graphene oxide modified graphite electrode was successfully developed for the simultaneous determination of morphine and methadone. The electrode process was investigated by cyclic voltammetry (CV) and differential pulse voltammetry (DPV). Nanocomposite structure was characterized by FTIR and EDX and XRD. Taguchi's experimental design method was applied to determine the optimum operating conditions such as pH, bandwidth, scan rate, and buffer concentration. And according to the results, pH and buffer concentration were determined as the most effective parameters on the performance of the modified electrode. Under optimized conditions, the calibration curve for methadone presents two linear ranges of current versus analytes concentration in the range of 0.1 to 20 μM and 20 to 323 μM, and 0.05 to 350 μM for morphine, with the detection limits of 0.03μM. For methadone 0.04μM for morphine (3sb / B). The quantification limits and precision were found to be acceptable. Finally, the developed method was successfully applied for target analytes determination in blood sera taken from different volunteers.

1. INTRODUCTION

Morphine and methadone whose IUPAC systematic full names are (7,8-didehydro-4,5-epoxy-17-methyl(5α,6α)-morphinan-3,6-diol) and (Rs-6-(Dimethylamino)-4,4-diphenyl heptan-3-one) are known as drugs which have similar impacts such as analgesic, sedative, and detoxifying effects along with physical and psychological dependency [1] (see Figure S1).

Morphine is a natural opiate of the opium syrup with brands such as Epiorph, Duramorph, Astramorph which is derived from phenylethylamine, whereas methadone is a pure industrial agonist with Dolomite brand [2-5]. The addictive effect of methadone is less than that of morphine and Methadone has a longer lifespan than morphine [6], because due to lipophilicity it stays in the liver and other tissues and spreads slowly. That's why methadone, like morphine, is used today to treat drug addiction. Simultaneous use of this drug with some medicines may cause severe drug interaction and sometimes it can result in disruption of the central nervous system. Consequently, accurate measurement of methadone and morphine in blood and urine is important to prevent poisoning and death. The analysis of drugs in biological fluids has also been used in forensic and pharmaceutical studies [7,8]. There are many methods available today for measuring the amount of morphine and methadone.

There are several reports has been reported about analytical techniques and methods for determination Morphine and Methadone such as high performance liquid chromatography [9-12], gas chromatography–mass spectroscopy [13,14], gas chromatography [15-18], liquid chromatography [19-21], capillary electrophoresis [22-28], spectrophotometry [29-30], chemi-luminescence [31-33], ultraviolet spectroscopy [34,35], atomic absorption and atomic emission spectroscopy [28,36], electrochemical methods [37-43].

Among the various techniques mentioned, chromatography is one of the most commonly used methods. But due to the relatively high cost, long analysis time, the need for high purity materials, user skill, and in some cases low sensitivity, it has attracted less attention .

The electrochemical techniques are very well known because of their high selectivity, simplicity, high speed, high sensitivity, low detection limit, and reasonable price. The variety of electrodes has added to this popularity [44-46]. However, limitations such as interactions with other species in the real sample, contamination of the electrode surface, and slow electron transfer have led the electrochemists to modify the electrodes in the last decade. In this regard, recently various surface-modified electrodes have been considered. Nanoparticles such as graphene, graphene oxide, and synthetic carbon-based nanoparticles have been developed due to properties such as facilitating electron transfer, increasing the speed of slow electrochemical reactions, high stability, and low detection limits [47-50]. Among nanoparticles, quantum dots such as cadmium selenide, which is a semiconductor itself, can be used to identify biomolecules as another major candidate for electrode surface modification due to its small size, high electron conductivity, and good catalytic activity [51-54]. Graphene oxide, with its unique mechanical, electrical, and optical properties, is also capable of providing a large

surface area suitable for conducting electrochemical reactions with optimum conductivity. Among Graphene and its derivatives, reduced graphene oxide is eight times more common than graphene oxide to modify the electrode surface due to its better electrical conductivity [55-58]. The simultaneous use of quantum dots of cadmium Selenide and graphene oxide at the electrode surface has led to the unique properties of the two groups being merged and a new function created due to its modification with Graphene oxide and nanoparticles. Due to the simple preparation process, high sensitivity, structural stability, and interesting electrical properties of quantum dots, the use of these compounds can offer new and applicable potential for the creation of robust sensors for the desired analytes and many important species.

In light of these considerations, the present study was conducted using thioglycolic acid decorated CdSe doped graphene oxide multilayers deposition on the pencil graphite electrodes (PGE) to provide a new electrochemical sensor as a working electrode for simultaneous determination of morphine and methadone .

Considering the effect of some important parameters on the efficiency of the method and determination of the optimum experimental conditions for simultaneous measurement of two analytes and designing the test in Taguchi method to optimize the chemical process, the sum of the factors leads to a systematic approach. Its benefits include cost and time reduction and designing a simpler and more efficient way to extract and measure target analytes [58]. Although there is a great deal of research on measuring methadone and morphine separately, library research shows that simultaneous measurement of these two compounds has not been reported with the help of such sensors. On the other hand, because methadone is used to improve the health of opioid addicts, by measuring methadone and morphine levels in the blood, it is possible to find out the process of recovery and the amount of this substance in the body.

Given the advantages of electrochemical methods, electrode surface modification, and experimental design, the main objective of the present study was to fabricate an electrochemical sensor with acceptable selectivity and high sensitivity for simultaneous detection of methadone and morphine in real biologic samples matrix.

2. EXPERIMENTAL

2.1. Chemicals

All chemicals including ethanol, graphite, potassium permanganate, sodium chloride, disodium hydrogen phosphate, sodium dihydrogen phosphate, oxygenated water, hydrochloric acid, phosphoric acid, were obtained from Merck Company (Darmstadt, Germany) without any purification.

High purity morphine sulfate and methadone (99%) were obtained from Darupakhsh Company (Tehran, Iran). Double-distillation water (ddH$_2$O) was used in all experiments where the electrical conductivity of the super-pure water was $10^{-6} \times 5.5$ MΩ.CM^{-1} [59].

The stock solutions of analytes were prepared in pure ethanol. Methadone and morphine stoke solutions had a concentration of 1000 ppm respectively. Phosphate buffer solution 0.1 mol L^{-1} was prepared at different pH with double distillation water (ddH$_2$O).

2.2. Devices

The electrochemical experiments performed in this study were performed using a Polarograph Metrohm device model 797 VA Computrace, (Switzerland) consisting of three electrodes, an Ag /AgCl (saturated KCl) electrode as the reference electrode, a platinum wire as the auxiliary electrode, and a modified pencil graphite electrode (PGE; brand Know 2B, with an internal thickness of 0.7 mm and length of 9 cm) was used as the working electrode.

Provided samples from designed sensors were characterized. The electrode was dried before recording XRD patterns. The analysis by using Energy Dispersive X-ray Spectroscopy (EDS) was performed by a silicon drift detector which was used to collect and count the number of X-rays emitted at each energy level. The FT-IR device was used to record IR spectra. Structural investigations were performed by X-ray diffraction (XRD) with a Siemens D500 diffractometer (Er- Langen, Germany, Cu-Kα radiation) with a wavelength of 1.54056 Å to obtain the spectra in a range of 20° to 90° in 2θ angle. Field emission scanning electron microscopy, FESEM, MIRA3, (TESCAN, Czech Republic) was used to determine surface morphology.

The ultrasonic processor model UTR200 (Hielscher, Germany) has been used to synthesize cadmium selenide. The pH adjustment of the solutions was carried out using the pH meter Laboratory Model 827 of Metrohm Brand (Switzerland).

2.3. Nano adsorbent synthesis and electrode fabrication processes

2.3.1. Thioglycolic acid (TGA) bonded cadmium selenide quantum dots

Synthesis procedure was adapted from reference [60] with slight modifications and included the following steps. 0.4567 g (2 mmol) of aqueous cadmium chloride (CdCl$_2$.2.5H$_2$O) was dissolved in 100 ml distilled water and poured into a 250-liter three-spout flask. 0.5 ml of thioglycolic acid was added to it. The flask containing the material was placed on a magnetic stirrer/hot plate and the solution was stirred for several minutes until it was uniform. Then, the pH of the solution is raised to 11 by 0.1 M sodium hydroxide and nitrogen gas passes through it to eject oxygen and other interfering gases. After a few minutes, 0.1 g of sodium borohydride (NaBH$_4$) and 0.111 g of selenium dioxide was added to it and the resulting solution refluxed. Thereby, the TGA-capped CdSe QDs were synthesized.

2.3.2. Graphene oxide preparation

Graphene oxide was synthesized according to the modified Hummers method. For this purpose 2.0g of graphite powder was added to 45.0 mL of concentrated sulfuric acid in the ice bath (about5.0 degrees) and medium speed for 2 h. After increasing the temperature to 15 °C, 1.0 g sodium nitrate was added to the mixture, allowed to stir for 30 minutes. Then,6.0g of potassium permanganate was carefully added while the aqueous solution was kept in a cold-water bath and the temperature was controlled at 20 ° C. Boiling water was added to the bath until the solution temperature reached to 35 °C. The mixture was stirred at a temperature of 35 °C for 2 hours. After this period, the container was placed in a water bath and 100 ml of deionized water was added to it while stirring and was kept at 90 ° C for 30 min. Then 10 ml of hydrogen peroxide (H_2O_2) 30% and 150.0 ml of deionized water were added to the previous mixture. Then, bubbling occurred and a bright yellow color was observed. This implied a high oxidation rate.

The solution was then filtered using the filter paper to remove the metal sulfate and a graphite oxide was produced. The graphite oxide was washed with 5% HCl aqueous solution until the sulfate ions were removed completely. The washing process was repeatedly performed together with centrifugation, and the supernatant was decanted away. The pH of the collected material was checked. The collected graphite oxide was stirred in distilled water at 60°C for 12 hours in a water bath. Finally, 160 ml of deionized water was added to the graphite oxide and the suspension was stirred under ultrasound for 1 to obtain single-layer graphene oxide (GO). Ultrasonication treatment also confirms the enhanced oxidation effect. This procedure is called exfoliation. Then, the synthesized GO powder was collected by centrifugation and dried at 60°C for 24 hours [61].

2.3.3. Preparation of the modified electrode

A simple three-step electrochemical approach was used to modify the PGE. The pencil graphite rods were first rinsed with deionized water for ten minutes. It was then rinsed with acetone for ten minutes to remove fat and possible organic impurities. After rinsing again with deionized water, the graphite rods dried.

Then, in the second step, 0.002 g of synthesized graphene oxide was immersed into 10 ml of deionized water and the suspension was stirred for ten minutes under ultrasonic waves to obtain a dispersed solution. The graphite rods were then placed in the solution for 6 hours. Over the surface of the as-prepared PGE, the GO was performed using the deep coating method. Then the PGEs were removed from the solution and placed at room temperature for one day to dry. In this way, the step of covering the PGEs with graphene oxide was done.

In the third step, TGA capped CdSe QDs solution was prepared by adding 0.002 g of it in 10 ml of deionized distilled water. The solution was sonicated for ten minutes. Electrodes with graphene oxide coating were placed inside the solution for 6 hours, along with continuous

stirring of the solution. The electrodes were then removed and dried for one day at room temperature. Thus, the step of covering the PGEs with TGA@CdSe/GO was done.

3. RESULTS AND DISCUSSION

3.1. Characterization of the synthesized nanomaterials

XRD, EDS, SEM, and FT-IR were used to characterize the cadmium selenide quantum dots capped by TGA-capped CdSe QDs. The crystal structure and crystallite size of the synthesized nanoparticles were investigated by generating diffraction patterns, from the crystalline powder samples at ambient temperature. The X-ray diffraction (XRD) pattern of the cadmium selenide quantum dots is shown in Figure 1. Maximum observed scattered peaks are in accordance with the joint committee on powder diffractions standards (JCPDSNo. 19-0191). The most top peaks are in (111), (220), (311) directions in 2θ =26.14°, 43.156 °, 49.13° respectively, and indicating the products are zinc-blende CdSe.

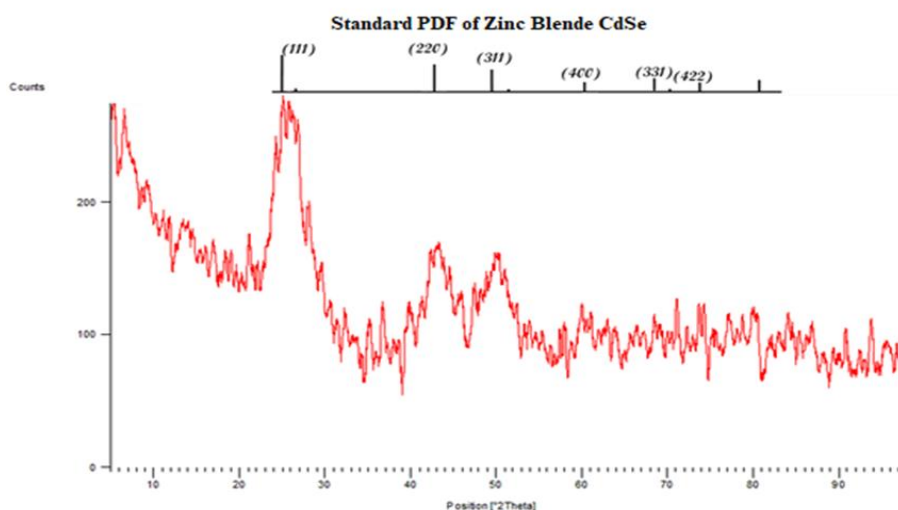**Figure 1.** XRD pattern of TGA capped CdSe QDs

The mean crystalline size can be calculated using the Debye-Scherrer equation ($D = k\lambda/\text{ß}\cos\theta$) where k is called the Scherrer's constant, the value of which is often assumed to be 0.9, λ is the wavelength of the X-ray radiation (Cu Kα radiation with λ=1.54056 Å was used.), θ is the Bragg diffraction angle (2θ range of 5°–99°), and ß is the full-width at half-maximum (FWHM) [62-66]. The average crystalline size of CdSe nanoparticles was determined from the FWHM of the (111) reflection of the XRD pattern using the Debye-Scherrer equation. The calculation showed that the average crystalline size is 4.15 nm.

The chemical composition of the synthesized CdSe QDs was investigated with EDS. The results are shown in Figure 2 confirmed that Cd and Se were present. The presence of sulfur and oxygen in the composition confirms the existence of TGA in this structure. The calculated

atomic ratio of Cd to Se shows to be close to 2:1. The elements obtained in the EDS analysis are summarized in Table S1(presented in the supplementary file).
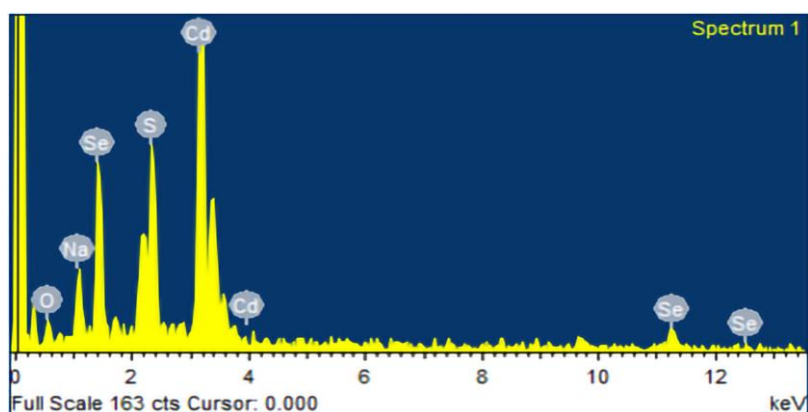

Figure 2. EDS spectra of CdSe capped with TGA

FT-IR spectroscopy prepared information about the bonds that originated between the surface coatings and the CdSe surface. For interpretation, Figure 3 contains the FT-IR spectra of the CdSe QDs stabilized with TGA. Additionally, Figure 3 provides the assignment of the main FT-8jIR band and offers a scheme that represents how TGA binds to the CdSe QDs.
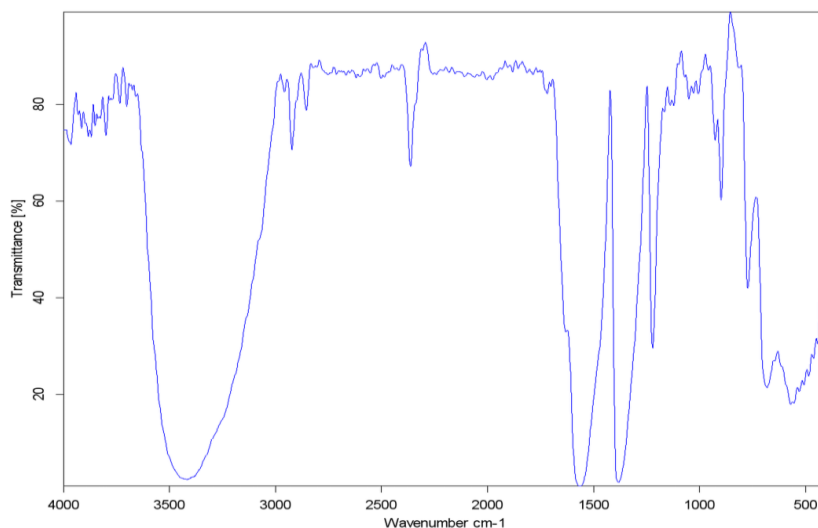

Figure 3. FT-IR spectra from CdSe capped with TG

The peaks of the capped CdSe samples between 1600–1650 cm^{-1}showed the absorption bands assigned to the carboxylate anion of the TGA (symmetric and asymmetric stretching vibrations). The existence of the carboxylate anion in the CdSe QDs resulted from the adjust the pH of the solution to 11.0 in the synthesis process and therefore deprotonated the COOH group. The O–H stretching of absorbed water appeared as a broad band in the region of 3250–

3420 cm^{-1} in the spectra of TGA-capped CdSe QDs. It was expected that an absorption band would appear around 2500 cm^{-1} due to the thioglycolic acid S-H group. This peak disappeared in the case of the TGA-capped QDs, indicating that the TGA attached to the surface of CdSe QDs via its sulfur atoms. Also, the Cd-Se band stretching should have been observed at ~720 cm^{-1}. However, for the reasons mentioned this peak is very weak. It can be distinguished the peaks appear in graphite oxide (Figure S2A) at 3400 to 3520, 1725, 1625, 1390, 1225 and 1100 cm^{-1} due to –OH stretching, C=O (carboxyl) stretching, C=O, –OH bending, C- OH stretching and C-O stretching vibrations.

The results of graphene oxide FTIR are shown in Figure S2B. Graphene oxide exhibited vibrational bands at 1051 cm^{-1}, 1723 cm^{-1}, and 3000 to 3600 cm^{-1}, due to the presence of typical oxygen functional groups, C–O–C, C=O, and O–H respectively, and the peak observed at 1625 cm^{-1} is attributed to C–C stretching vibration.

The morphology of GO/PGE and TGA@CdSe/GO/PGE were studied by SEM (Figure 4). The SEM images demonstrated that the NPs distributed homogeneously across the electrode surface.

The response of an electrochemical sensor is related to its physical morphology. In order to characterize GO deposited on the PGE surface, the SEM analysis was carried out on the surface of modified electrodes. For more information, the SEM images from the surface of bare PGE, GO powder, TGA@CdSeQDs powder, were shown by an electron microscope in Fig. S3 (a and c). The bare PGE surface before any modifications is shown in Figure S3-a. Figure S3-b shows that graphene oxide consisted of multiple graphene sheets. The morphology and structure of CdSe QDs were studied too in this manner (Figure S3-c).
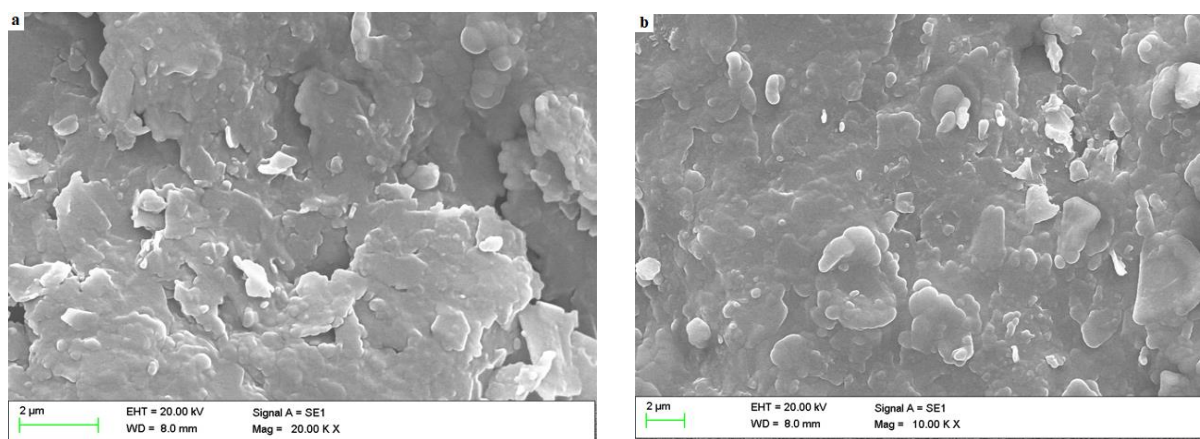

Figure 4. SEM images from the surfaces of (a) GO modified PGE, (b) CdSe/GO/PG

3.2. Electrochemical study

The electrochemical behavior of morphine and methadone under optimum conditions in saline phosphate buffer (pH = 7) and scan rate of 0.25 mV. S^{-1} (Figure 5) is irreversible and the oxidation peaks of these two substances (methadone in 0.74 and morphine in 0.42 V) were

observed using the modified PGE. Figure 5a shows DPV and 5b shows cyclic voltammetry in the presence of 10 mg.L^{-1} of each of the morphine (35 µM) and methadone(32 µM). CV graph shows two oxidation peaks at +0.74 V and +0.42V for methadone and morphine, respectively. As a result, the multi-layers of graphene oxide present with greater electrochemical capacitance than graphite in the bare PGE. On the other hand, metallic nano-compounds can exhibit high specific capacitance through the redox reactions at the interface of the electrode/electrolyte. Thus, CdSe due to electronic properties that arising from the composition, structure and very small sizes of quantum dots has a great effect on the transfer of electrons in the fabricated sensor. The QDs ability to transport electric currents is of great importance in the electrochemical process. The results confirm the increased sensitivity in the presence of the QDs modified electrode. All the measurements were carried out at room temperature (25.0±0.1 °C).
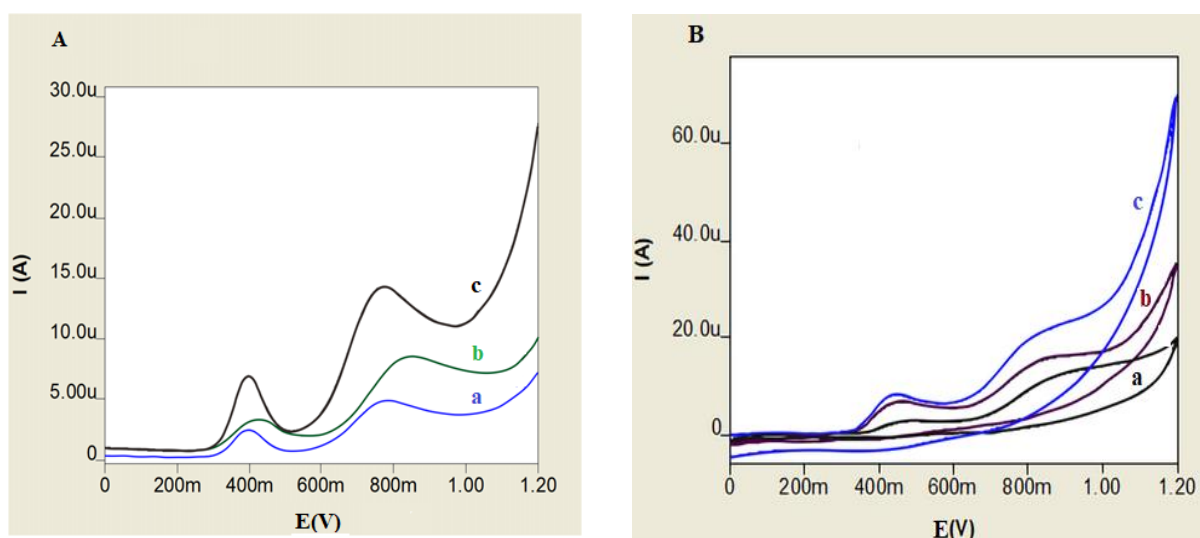

Figure 5. (A) Differential pulse and (B) cyclic voltammograms of methadone, and morphine at 10 mg.L^{-1} using: (a) a bare PGE (b) graphene oxide coated PGE and (c) GO/CdSe / PGE in the presence of 0.1 molar silane phosphate buffer (pH = 7) ,and scan rate of 0.25 mV.S^{-1}

In all electrochemical measurements, the TGA@CdSe/GO/PGEs were subsequently pretreated electrochemically in a potential window -0.2 to +1.2V, versus an Ag /AgCl reference electrode. The background signal was recorded for the blank in the absence of the analytes. No response in the absence of morphine and methadone was observed (See Figure S4).

3.3. Experimental design

The effect of the factors involved in this study has been investigated in two ways. In the first step a number of factors such as graphene oxide and CdSe amounts, and type of buffer electrolyte were optimized by changing one factor at a time and keeping other variables

constant (see Table 2). Other quantitative factors such as buffer concentration, pH, PGE modifier deposition period, and scan rate were studied by Taguchi approach [67]. Factors such as deposition time, graphene oxide concentration, CdSe concentration, and type of the buffer were optimized. As shown in Table S2, 6 h. deposition time, graphene oxide amount 0.002 gr, CdSe amount 0.002 gr, and saline phosphate buffer are the optimum values.

Table 1. ANOVA table for Taguchi approach

Source	d_f[a]	Ssd[b]	MS[c]	Adj MS	F-Value	P-Value
Buffer concentration (mg.ml^{-1})	4	89.121	89.121	22.280	15.20	0.001
pH buffer	4	11.879	11.879	2.970	2.03	0.183
Equilibration time (s)	4	3.023	3.023	0.756	0.52	0.727
Scan rate (V.s^{-1})	4	2.467	2.467	0.617	0.42	0.790
Residual error	8	11.723	11.723	1.465		
Total	24	118.213				

S = 1.21054   R-Sq = 90.08%   R-Sq (adj) = 70.25%
[a] Degree of freedom
[b] Sum of squares
[c] Mean Squares

3.3.1. Taguchi method design of experiments

Taguchi method experimental design is used to optimize the parameters under investigation for the sensor performance evaluation. Taguchi is a powerful tool for obtaining data in a controlled way to find the most effective factors that are performed by experimental design [69]. Taguchi, as an orthogonal array design, adds a novel aspect to conventional experimental design. In this method, more factors can study with a lesser number of experiments using orthogonal arrays.

Therefore, in this study, we used the Taguchi method through the two-step Minitab (16) software to identify the optimal parameters and select the most effective parameters. Also, all the main factors and two-factor interactions can be estimated by analysis of variance (ANOVA). To achieve this approach, each experiment was repeated three times, and means responses were calculated for each factor at different levels.

Important and effective parameters such as buffer concentration, pH, deposition time, and scan rate were investigated (See Figure S5). As a result, the most effective factors are the buffer concentration and pH of the buffer. The sum of squares of main and sub-effects and total variance and P values are listed in ANOVA (Table 1). The significance level P-value is reported in Table 1. In this analysis, F is equal to the ratio of the mean square error to the residual error

to determine the significance of a factor. The buffer concentration with 83.03% is the most effective factor and the scan rate with 2.3% is the least effective factor.

3.3.2. Analytical performance

Calibration graphs were constructed under optimum conditions of saline phosphate buffer (pH = 7) and a scan rate of 0.25 mV^{-1}. The calibration curves and equations are depicted in Figure S6. The statistical results of morphine and methadone measurements (n = 5) are reported separately in Table 2. To evaluate the practical application of the nanosensor, the merits such as correlation coefficient (R^2), corresponding regression equation (slope of calibration curve indicating sensitivity), limit of detection (LOD), and linear dynamic range (LDR) were investigated under optimal conditions.

Table 2. Statistical results of morphine and methadone studies

Statistical calculations	Morphine	Methadone
LDR[a] (μM)	0. 05-323	0.1-20 20-350
Calibration Equation (μM)	Y=0.038X+0.338	Y=0.069X+0.231 Y=0.032X+0.656
R^{2} [b]	0.9985	0.999 0.997
$S_{Y/X}$ [c]	0.048	0.011
S_b [d]	0.000676	0.00066
S_a [e]	0.0103	0.0058
Slope confidence limit	0.038±0.00173	0.069±0.0016
Intercept confidence limit	0.338±0.04	0.231±0.014
F Test	0.0385	2.8324E-07
T Test	0.0145	0.017
LOD[f]	0.038	0.0268
RSD[g]% (n=3)	2.78	1.28

[a] Linear dynamic range
[b] Correlation coefficient
[c] Statistic
[d] Standard deviation of slope
[e] Standard deviation of intercept
[f] limits of detection
[g] Relative standard deviation

Five measurements were taken at each level. According to the IUPAC (International Union of Pure and Applied Chemistry) official recommendations the LOD formula is: $LOD = Z + 3\bar{\delta}$ where Z is the average blank signal and δ is the average standard deviation of blank (n=7). According to the findings, the morphine signal increased linearly in the range of 0.05-323 μM and the methadone linear ranges are 0.1-20 and 20-350 μM.

According to the statistical rules, $S_{Y/X}$ estimates a random error in the(y), direction. Sd, represents the standard deviation of the slope, and Se is the standard deviation of intercept. The confidence intervals for the slope (B) and intercept (A) of least-squares regression lines are obtained from the relations B $\pm$t (n-2) $_{(n-2)}$ Sb and A $\pm$t (n-2)$_{(n-2)}$ Sa, and *n* is the number of data. The two-sample T-test is also used to determine whether the difference between means found in the sample is significantly different from the hypothesized difference between means.

If the two-sample T-test is statistically less than 0.05, their averages can be assumed to be equal. F-test is used to compare two population variances. If the obtained value is less than 0.05, it can be assumed that the variances of the two groups are the same.

The DPV result of the simultaneous changes in methadone and morphine concentrations is also shown in Fig. S6. Sensor response efficiency's remained unchanged for one week and then it decreased to 99% after ten days and to 97.9% after 20 days. To investigate the reproducibility, two other different modified PEGs were selected from OWNER (Korea) and TOUCHLNE (China). All PGEs were labeled in the same condition and the RSD% results were equal for the three measurements. Concentrations were the same 35.00 μM for morphine and 32.31 μM for methadone indicating its high reproducibility.
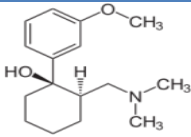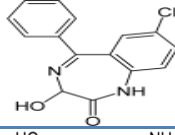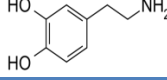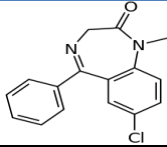
The relative standard deviation (RSD%) for the responses between electrodes (for Owner PGE) was 1.89% for morphine and 3.92% for methadone and (for TOUCHLNE PGE) was 1.98% for morphine and 3.75% for methadone and RSD% in this work (for TGA@CdSe/GO/PGE) was 1.85% for morphine and 3.75% for methadone respectively. The results showed that the reproducibility of the sensors for the determination of methadone and morphine are acceptable.

3.3.2.1. Investigating the selectivity effect

In order to evaluate the selectivity of the CdSe-GO-GPE sensors for the determination of morphine and methadone, the influence of some common interferences drugs namely tramadol, oxazepam, diazepam, and dopamine on the current response of the analytes under the optimum conditions were investigated.

The tolerance limit for interfering species was studied as the maximum concentration that gave a relative error less than 5.0% at a concentration of 30.0 μM of the target analytes. The tolerance limits for the interfering drugs were shown in Table 3. A comparison is made between the analytical aspects of the current nanosensor and some previous techniques for the determination of morphine and methadone, (See Table 4). This comparison with previous similar works showed that the TGA@CdSe/GO/PGE method has a reasonable detection limit, an acceptable linear dynamic range, and better selectivity.

Table 3. Investigating the selectivity effect

Drugs	Structure	pk$_a$	Log p[a]	Tolerance limit (morphine) (µM)	Tolerance limit (methadone) (µM)	RSD% (n=3)
Tramadol		9.41	2.4	10	300	3.5
Oxazepam		10.94	2.22	300	1	3.06
Dopamine		10.01	0.03	200	1	3.82
Diazepam		3.4	2.82	1	1	2.82

[a] Lipophilicity (LogP), the partition coefficient of a molecule between octanol and water

Table 4. An analytical comparison of the current method and some previous techniques on

the determination of morphine and methadone

Working electrode	Method	Linear range Morphine (µM)	LOD Morphine (µM)	Recovery Morphine	Linear range Methadone (µM)	LOD Methadone (µM)	Recovery Methadone	Ref.
Au/PEDOT/Au nanoSDS[a]	CV	2-18	0.428	99.8-101.9	-	-		[37]
MCNP/SPCE[b]	DPV	0.1-600	0.02	98 102.7	-	-		[68]
dsDNAb/SPCE[c]	EME-DPV	0.25-40	0.07	98-102	-	-		[69]
Fmwnt/GCE[d]	DPV	-	-		0.5 – 100	0.35	97.1-100.4	[43]
MWCNT/PGE[e]	DPV				0.1-15	0.087	95.66 102.4	[42]
GNPS/MWCPE	SWV				0.1-500	5	97.4 103	[41]
GO/CdSe-PGE	DPV	0.05-350	0.0138	98.36-102.67	0.1-20 20-323	0.264	98.77-102.1	This work

[a] Poly(3,4-ethylene-dioxythiophene)/Gold-nanoparticles
[b] Magnetic core shellmanganese ferrite nanopartical modified screen printed electrode
[c] Screen printed carbon electrode strips (SPCE) modified by double strand (ds) calf thymus DNA.
[d] Functionalized multi-walled carbon nanotubes
[e] Multi-walled carbon nanotubes modified pencil graphite electrode

3.4. Application of the presented method in real sample analysis

Blood samples were drawn from 3 healthy laboratory volunteers. Serum samples were prepared from whole blood samples using a method that has been commonly used in clinical laboratories [70]. We received the prepared serum from a medical diagnostic laboratory.

Table 5. Analytical results for simultaneous determination of methadone and morphine in serum samples

Blood serum sample	Added (µM)	Found ± δ (µM)	RSD%[a] (µM)	RR%[b]	Bias%
Morphine					
Sample # 1	0	0	0	0	0
	0.1	0.09906±0.0016	1.64	99.06	0.94
	0.3	0.308±0.0081	2.62	102.67	2.67
	0.6	0.5977±0.0167	2.98	99.62	0.38
	0.8	0.798233±0.0217	2.72	99.78	0.22
	1	0.9964±0.0232	1.08	99.64	0.36
Sample # 2	0	0	0	0	0
	0.1	0.09988±0.0021	2.1	99.88	0.12
	0.3	0.2968±0.0097	3.28	98.93	1.07
	0.6	0.603±0.0139	2.28	100.50	0.5
	0.8	0.7985±0.0188	2.35	99.82	0.18
	1	0.9993±0.0176	1.76	99.90	0.1
Sample # 3	0	0	0	0	0
	0.1	0.0996±0.0021	2.1	99.59	0.41
	0.3	0.2951±0.0048	1.64	98.36	1.64
	0.6	0.601±0.006835	1.14	100.17	0.17
	0.8	0.7992±0.0122	1.52	99.90	0.1
	1	0.9998±0.018	1.80	99.98	0.02
Methadone					
Sample# 1	0	0	0	0	0
	0.1	0.09934±0.001041	1.05	99.34	0.66
	0.5	0.49495±0.0050	1.020	98.99	1.01
	1	0.9985±0.0089	0.89	99.85	0.15
	1.5	1.52±0.02	1.31	101.33	1.33
Sample# 2	0	0	0	0	0
	0.5	0.4995±0.0097	1.94	99.90	0.1
	1	1.021±0.027	2.67	102.10	2.1
	1.5	1.491±0.034	2.26	99.40	0.6
	2	1.9838±0.02	1.02	99.19	0.81
Sample# 3	0	0	0	0	0
	0.5	0.49855±0.0081	1.63	99.71	0.29
	1	0.9877±0.019	1.96	98.77	1.27
	1.5	1.518±0.036	2.39	101.20	1.2
	2	1.9976±0.022	1.12	99.88	0.12

[a] Relative standard deviation
[b] Relative recovery

Then, the serum preparation method involved adding 2 volumes of HPLC grade ACN (400 μL) to 200 μL serum, centrifugation at 3500 rpm for 10 min, and allowing to stand at room temperature for 30 min. An aliquot of the supernatant was stored at 4.0 ^{0}C until used. In this work, we used acetonitrile (ACN), which has been shown to effectively precipitate proteins. ACN is a superior solvent to remove serum albumin and immunoglobulins from serum.

Under the optimum conditions, the electrochemical sensor was applied for the determination of morphine and methadone in the human serum samples. Due to the complexity of the serum matrix, the standard addition method was used determination of target analytes in a serum sample. As such, 1 ml of serum was added to the solution containing varying amounts of morphine and methadone (0.1, 0.3, 0.6,0.8, and1.0 μM) and then diluted with saline phosphate buffer (pH 7). The results of the study, along with the relative recovery, are listed in Table 5.

The acceptable recovery percentages obtained in the range of 98.36 to 102.67 with a standard deviation of 0.89 to 3.28 indicate that the electrochemical response of the designed sensor is not affected by the sample matrices and the proposed method is applicable for simultaneous determination of morphine and methadone in serum samples.

4. CONCLUSION

This work describes the construction process of a novel electrochemical sensor for the determination of methadone and morphine using TGA@CdSe/GO core-shell quantum dots nanocomposite which is deposited on the pencil graphite electrode surface. Sensitive methadone and morphine detection were obtained due to facile electron transfer between the adsorbent selective recognition cavities, which readily captured analytes in a suitable confirmation and the superior properties of TGA@CdSe core-shell quantum dots nanocomposite. Due to their quantum confinement, edge effects, and large surface area, QDs are very efficient for the immobilization of increased loadings of some materials by simple adsorption, covalent immobilization, etc. It is notable that the rapid response and easy detection of the analytes are the great features of the quantum dot based fabricated sensor. Overall, this sensor presented a simple and reliable method to detect opium with wide potential applications.

REFERENCES

[1] M. Vazirian, and G. Mostashai, Strategies and Applications of Drug Abuse Treatment, Ministry of Health and Medical Education with Secretariat of the Anti-Narcotics Headquarters, Parshkooh Publications, Tehran.

[2] A. Ferrari, Pharmacological Res. 5 (2004) 551.

[3] M. J. O''Neil (ed.), The Merck Index - An Encyclopedia of Chemicals, Drugs, and Biologicals. Cambridge, UK: Royal Society of Chemistry (2013) pp. 1116.

[4] W. M. Haynes, Clin. Pharmacol. Ther. 47 (1990) 12.

[5]   R. Osborne, S. Joel, D. Trew, and M. Slevin, Clin. Pharmacol. 47 (1990) 12.

[6]   S. Khalil, and A. Kelzieh, J. Pharm. Biomed. Anal.13 (2003) 601.

[7]   A. Salimi, R. Hallaj, and G. R. Khayatian, Electroanalysis 56 (2005) 185.

[8]   A. Ensafi, A. Karimi-Maleh, Electroanalysis.115 (2010) 256.

[9]   Q. C. Meng, M. S. Cepeda, T. Kramer, H. Zou, D. J. Matoka and J. Farrar, J. Chromatogr. B 74 (2000) 2115.

[10]   F. Tagliaro, D. Franchi, R. Dorizzi, and M. Marigo, J. Chromatogr. 488 (1989) 215.

[11]   M. Franke, C. L. Winek, and H. Kingston, Forensic Sci. Int. 81 (1996) 51.

[12]   S. Rudaz, and J. L. Veuthey, Pharm. Biomed. Anal. 141 (1996) 271.

[13]   T. Hyotyloinen , H. Keski-Hynnila, M. L. Riekkola, J. Chromatogr. A 771 (1997) 360.

[14]   S. Khalili, M. El-Ries, J. Pharma. Biomed. Anal. 27 (2002) 117.

[15]   M. H. Lee, C. W Lee. J. Anal. Toxicol. 15 (1991) 182.

[16]   T. S. Ho, S. Pedersoen – Bjergaard, and K. E. Rasmussen, J. Chromatogr. (2002) 9633.

[17]   F. Ahmadi, H. Rezaei, and R. Tahvilian, J. Chromatogr. 9 (2012) 1270.

[18]   H. Ebrahimzadeh, F. Mirbabaei, A. A. Asgharinezhad, N. Shekari, and N. Mollazadeh, J. Chromatogr. B 94 (2014) 775.

[19]   G. Ghari, A. Gulati, R. Bhat, and I. R. Tebbett, J. Chromatogr. 57 (1991) 1263.

[20]   L. Somaini, M. A. Saracino, C. Marcheselli, S. Zanchini, G. Gerra, and M. A. Raggi, Anal. Chim. Acta 702 (2011) 280.

[21]   E. Ranjbari, A. A. Golbabanezhad–Aziz, and M. R. Hadijmohammadi, Talanta 94 (2012) 116.

[22]   S. W. Lewis, P. S. Francis, and K. F. Lim, Analyst 125 (2000) 1869.

[23]   G. Sakai, K. Ogata, T. Uda, and N. Miura, Sens. Actuators Chem. B 49 (1998) 5.

[24]   R. B. Taylor, and R. G. J. Chromatogr. B 675 (1996) 213.

[25]   M. Macchia, G. Manetto, C. Mori, and C. Papi, J. Chromatogr. A. 924 (2001) 499.

[26]   Mi. JQ, X. X Zhang, and W. B. Chang. J. Immunoassay Immunochem. 25 (2004) 57.

[27]   J. L. Tsai, W. S. Wu, and H. H. Lee, Electrophoresis 21 (2000) 1580.

[28]   H. R. Lin, C. L. Chen, C. L. Huang, S. T. Chen, and A. C. Lua, J. Chromatogr. B 10 (2013) 925.

[29]   A. Sheibani, M. R. Shishehbove, and E. Mirparizi, Spectrochim. Acta A 77 (2010) 535.

[30]   E. Jack, and E. Horace, Analyst 9 (1972) 1397.

[31]   J. A. M. Pulgarin, L. F. G. Bermejo, J. M. L. Gallego, and M. N. S. Garica, Talanta 74 (2008) 1539.

[32]   A. M. Idris, and A. O. Alnajjar, Talanta77 (2008) 522.

[33]   X. Zhang, and A. J. Bard, J. Phys. Chem. 92 (1988) 5566.

[34]   M. E Soares, V. Seabra, and M. L. Bastos, J. Liq. Chromatogr. 15 (1992) 1533.

[35]   R. L. Sinsheimer, and J. F. Scott, Institute of Technol. Cambridge (1950) 299.

[36]   I. Heitaroh, and K. Watanabe, J. Pharmacol. 21 (1971) 731.

[37] N. F. Atta, A. Galal, and E. H. El-Ads, Int. J. Electrochem. Sci. 9 (2014) 2131.

[38] K. C. Ho, C. Y. Chen, H. C. Hsu, L. C. Chen, S. C. Shiesh, and X. Z. Lin, Biosens. Bioelectron. 3 (2004) 20.

[39] W. M. Yeh, and K. C. Ho, Anal. Chem. Acta 76 (2005) 542.

[40] F. Xu, M. N. Gao, and L. Wange, Talanta 58 (2002) 427.

[41] A. Afkhami, F. Soltani-Felehgari, and T. Madrakian, Talanta 128 (2014) 203.

[42] E. Alipour, M. R. Majidi, and O. Hoseindokht, J. Chinese Chem. Soc. 62 (2015) 461.

[43] M. Amiri-Aref, J. B. Raoof, and R. Ojani, Coll. Surfaces. B 109 (2013) 287.

[44] R. Pourtaghavi, and M. H. Mashhadizadeh, Talanta 131 (2015) 460.

[45] A. Niazi, and A. Yazdanipour, Chem. Lett.19 (2008) 465.

[46] M. H. Pournaghi-Azar, and A. Saadatirad, J. Electroanal. Chem. 624 (2008) 293.

[47] S. Z. Mohammadi, and H. Beitollahi, J. Anal. Chem. 73 (2018) 716.

[48] G. Karim-Nezhad, Z. Khorablou, and P. SeyedDorraji, Int. J. Nano Dimens. 9 (2018) 314.

[49] E. A. Gomaa, M. A. Morsi, A. E. Negm, and Y. A. Sherif, Int. J. NanoDimens. 8 (2017) 89.

[50] J. Cassidy, J. Ghoroghchian, F. Sarfarazi, and J. J. Smith, Electrochim. Acta 31 (1986) 629.

[51] X. G. Peng, M. C. Schlamp, A. V. Kadavanich, and A. P. Alivisatos, J. Am. Chem. Soc. 119 (1997) 7019.

[52] F. Ye, A. Barrefelt, H. Asem, and M. Abedi-Valugerdi, Biomaterials. 35 (2014) 3885.

[53] Y. Su, Y. He, H. Lu, L. Sa, Q. Li, W. Li. L. Wang. P. Shen, and Q. Huang, Biomaterials 30 (2009) 19.

[54] L. Tang, G. M. Zeng, G. L. Shen, Y. P. Li, Y. Zhang, and D. L. Huang, Environ. Sci. Technol. 42 (2008) 1207.

[55] M. Zhou, Y. L. Wang, Y. M. Zhai, J. F. Zhai, and W. Ren, Chem-Eur. J. 15 (2009) 6116.

[56] T. Mueller, F. N. Xia, and P. Avouris, Nature Photonics 4 (2010) 297.

[57] H. Xu, H. Dai, and G. Chen, Talanta 81 (2010) 334.

[58] C. C. Chan, W. C. Hsu, C. C. Chang, C. S. Hsu, Sens. Actuators B 145 (2010) 691.

[59] R. M. Pashley, M. Rzechowicz, L.R. Pashley, M. J. Francis, J. Phys. Chem. B 109 (2005) 1231.

[60] Y. Wang, Y. Mo, L. Zhou, Spectrochim. Acta A 79 (2011) 1312.

[61] S. Stankovich, Nature 442 (2006) 282.

[62] W. X. Zhang, C.Wang, L. Zhang, X. M. Zhang, X. M. Liu, K. B. Tang, and Y. T. Qian, J. Solid. State Chem.151 (2000) 241.

[63] M. J. Bowers, J. R. Bride, and S. J. Rosenthal, J. Am. Chem. Soc.127 (2005) 15379.

[64] D. W. Deng, J. S. Yu, and Y. J. Pan, J. Colloid Interface Sci. 299 (2006) 225.

[65] M. Behboudnia, Y. Azizianekalandaragh, Mater. Sci. Eng. B 138 (2007) 65.

[66] W. G. Chang, Y.H. Shen, A.J. Xie, H. Zhang, J. Wang, and W. S. Lu, J. Colloid Interface Sci. 335 (2009) 257.

[67] S. R. Rao, and G. Padmanabhan, Int. J. Eng. Res. Appl. 2 (2012) 192.

[68] H. Beitollahi, Z. Mohammadi, and S. Tajik, Int. J. Nano Dimens.10 (2019) 304.

[69] R. Feizbakhsh, M. Ebrahimi, and A. Davoodnia, International Journal of Medical Research & Health Sciences 5 (2016) 206.

[70] H. Chen, C. Yao-chang, Y. Zung, F. Shao-Tsu, Neuropsychiatric Disease Treatment 11 (2015) 609.